Total AC Interferences Between a Power Line Subject to a Single-Phase Fault and a Nearby Pipeline with Multilayered Soil

Caio M. Moraes
Gustavo H. de Sá Matos *
Amauri G. Martins-Britto
Kleber M. Silva
Department of Electrical Engineering
University of Brasília, UnB
Brasília, Brazil
{caiomoraes@lapse., amaurigm@, klebermelo@}unb.br, gustavodesamatos@gmail.com*

***Abstract*—This paper describes the problem of electromagnetic interferences between power lines and metallic structures, caused by inductive and conductive coupling mechanisms, and the main risks to which personnel and facilities are exposed. An EMTP-based implementation is proposed to predict induced voltage levels on a target circuit, due to interferences caused by overhead power lines under steady-state nominal load, as well as fault conditions, using generalized formulas to represent the N-layered soil. Results are tested by means of a case study of a real shared right-of-way project and comparisons with results obtained using industry-standard software. Results show that the proposed method is accurate, with errors smaller than 8%. Stress voltage values in the interfered pipeline are the order of 50 kV, exposing the structure coating to risk of breakdown, which may lead to corrosion and pipeline failure. A mitigation is designed and proven to reduce voltage values to safe levels, in compliance with the nominal limits from the manufacturer.**

***Index Terms*—Electromagnetic interferences, Electromagnetic Transient Program (EMTP), pipelines, single-phase fault and transmission lines.**

I. Introduction

Overhead transmission lines (TLs) are large structures and require large right-of-ways which often extend for several hundred kilometers. Due to the trend of sharing space with other facilities, forming the so called utility corridors, and the energy levels involved, TLs may induce currents in nearby metal structures that are not designed to conduct electricity. This effect may raise risks to metallic installations neighboring the TLs through three types of electromagnetic interference (EMI) mechanisms: inductive, conductive and capacitive couplings [1].

EMIs are influenced by current levels flowing through TL conductors, length of exposure, soil characteristics and constructive aspects of the facilities involved [1].

Serious design errors may occur if these EMI are not properly addressed, exposing personnel and installations to risks, which justifies the efforts in developing reliable and realistic simulation models.

EMI studies reported in the literature generally represent the soil as semi-infinite and homogeneous structure or represent N-layered soils by equivalent homogeneous models. This approach is reported to yield inaccuracies in a variety of practical cases, due to the multilayered characteristic of natural soils [2], [3], [4]. Moreover, to the best of the author's knowledge, there is no report in the specialized EMI literature accounting for arbitrary multilayered soil models within the EMTP-based paradigm.

This paper presents an EMTP-based implementation for inductive and conductive coupling studies caused by a TL under nominal load and phase-to-ground fault conditions with multilayered soil models.

Self and mutual impedance calculations are based on a generalized solution for overhead and buried conductors considering N-layered soils, proposed by Tsimiatros et al [5].

To properly account for earth conduction effects, the generalized N-layered Green's function, proposed by He et al. [6] and Li et al. [7], is used to represent the ground potential rise along the interfered structure, due to currents flowing into the soil under fault conditions.

The proposed implementation is leveraged to analyze the case of a real right-of-way in Brazil, shared between a 138 kV TL and an underground metallic pipeline. A 3-layered soil model is determined from local resistivity measurements. The proposed method is used to calculate the resulting stress voltages due to a phase-to-ground fault.

The obtained results are compared with software CDEGS and present RMS errors of less than 8% in the cases analyzed. Stress voltages in the pipeline coating yield values close to 50 kV, which subjects the installation to risks that must be addressed according to safety standards.

Then, further simulations are performed to design a mitigation solution to reduce stress voltage levels along the interfered pipeline, which is demonstrated to reduce the initial stress voltage approximately in 50%, thus ensuring compliance with industry standards.

II. Mathematical Model

A. Inductive coupling

Currents flowing in an energized conductor produces a time-varying magnetic field, as shown in Fig. 1. This time-varying magnetic field causes electromotive forces (EMFs) which, on their turn, induce voltages and currents on a metallic structure laid parallelly to the energized conductor. This electromagnetic phenomenon is known as inductive coupling [1].

The inductive influence of a transmission line conductor on a nearby pipeline depends on the current magnitude, distance between structures, exposure length, soil resistivity, as well as the characteristics of installations involved [1].

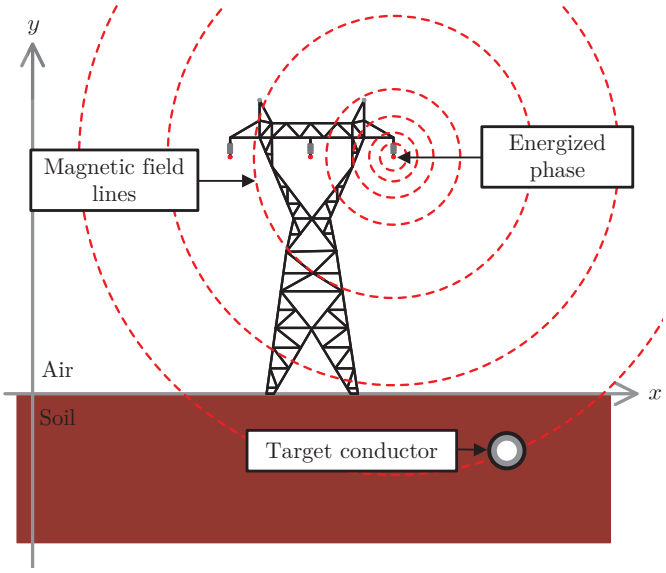

Fig. 1. Inductive coupling phenomenon, adapted from [8].

The induced EMF (E) is numerically given by [1]:

$$E = Z_m \times I \tag{1}$$

in which Z_m is the mutual impedance between the source and the target conductors, in ohms.meter; I is the current in the energized conductor, in ampères; and E is the EMF imposed to the target metallic structure, in volts per meter.

B. Mutual impedance for N-layered soil

The mutual impedance, described by term Z_m in (1), is calculated based on the generalized solution proposed by Tsiamitros et al. [5], which extends the well-known Carson's [9], Nakagawa's [10] and Pollaczek's [11] original formulas and is reported to accurately handle complex configurations composed of both overhead and buried conductors in or above N-layered earth, as well as the displacement current effects, thus covering a frequency spectrum up to 1 MHz.

Fig. 2 illustrates two conductors i and j in an N-layered earth structure, in which each layer is described by the corresponding parameters permeability (μ_i), permittivity (ϵ_i), conductivity (σ_i) and thickness (d_i). Conductors are depicted as buried in the m^{th} and l^{th} layers of the N-layered earth, respectively, for illustration purposes, with no loss of generality. The per unit length mutual impedance $Z_m = Z_{i,j}$ is calculated from (2), in which $\omega = 2\pi f$ is the angular velocity, in radians per second; h_1 and h_2 are the relative vertical distances to the upper boundaries of layers m and l, respectively, in meters; $y_{i,j}$ is the horizontal distance between conductors i and j, in meters; and $\bar{\alpha}_i = \sqrt{u^2 + \bar{\gamma}_i^2}$, $\bar{\gamma}_i^2 = j\omega\mu_i(\sigma_i + j\omega\epsilon_i)$, with $i = 0, 1, 2, \ldots, N$ [5].

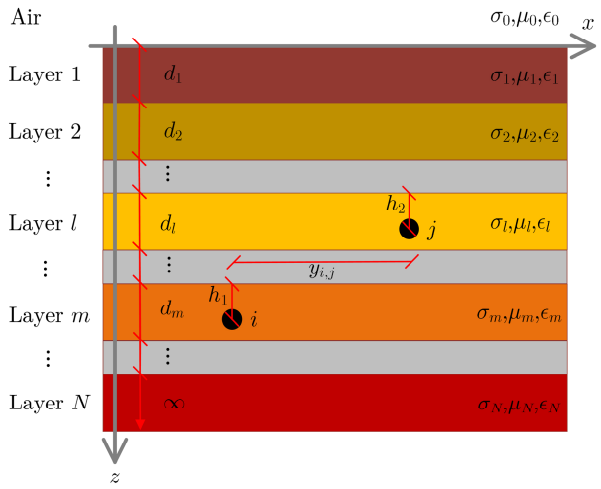

Fig. 2. Two underground conductors in N-layered soil.

Terms $D\bar{T}N_i$, $D\bar{T}D_i$, $T\bar{D}N_k$ and $T\bar{D}D_k$, given in (3)-(10), relate the electromagnetic and geometric characteristics of the successive layers, in which $i = 0, 1, 2, \ldots, N$ and $k = 0, 1, 2, \ldots, m$. Following the same notation as [5], the first characters of expressions TD ("Top to Down") and DT ("Down to Top") denote the direction of the recursive formulas, and the characters D ("Denominator") and N ("Numerator") indicate where each term usually appears during the formula expansion.

$$\begin{aligned} D\bar{T}N_i = {} & (\mu_{i+1}\bar{\alpha}_i - \mu_i\bar{\alpha}_{i+1})D\bar{T}D_{i+1} \\ & + (\mu_{i+1}\bar{\alpha}_i + \mu_i\bar{\alpha}_{i+1})D\bar{T}N_{i+1}e^{-2\bar{\alpha}_{i+1}d_{i+1}}, \end{aligned} \tag{3}$$

$$\begin{aligned} Z_{i,j} &= \frac{j\omega\mu_m}{2\pi}\int_0^\infty \frac{cos(uy_{i,j})}{\bar{\alpha}_m} \times \left\{ 2^{m-l}\frac{(\mu_1\mu_2\ldots\mu_{m-1})(\bar{\alpha}_1\bar{\alpha}_2\ldots\bar{\alpha}_m)(e^{-\bar{\alpha}_l d_l}e^{-\bar{\alpha}_{l+1}d_{l+1}}\ldots e^{-\bar{\alpha}_m d_m})}{(\mu_1\mu_2\ldots\mu_{l-1})(\bar{\alpha}_1\bar{\alpha}_2\ldots\bar{\alpha}_l)} \cdot \frac{\bar{F}_1\bar{F}_2}{D\bar{T}D_0} \right\} du, \\ \bar{F}_1 &= [D\bar{T}D_m e^{\bar{\alpha}_m(d_m - h_1)} + D\bar{T}N_m e^{-\bar{\alpha}_m(d_m - h_1)}], \\ \bar{F}_2 &= [T\bar{D}D_{l-1}e^{\bar{\alpha}_1 h_2} + T\bar{D}N_{l-1}e^{-\bar{\alpha}_1 h_2}]. \end{aligned} \tag{2}$$

$$D\bar{T}D_i = (\mu_{i+1}\bar{\alpha}_i + \mu_i\bar{\alpha}_{i+1})D\bar{T}D_{i+1} + (\mu_{i+1}\bar{\alpha}_i - \mu_i\bar{\alpha}_{i+1})D\bar{T}N_{i+1}e^{-2\bar{\alpha}_{i+1}d_{i+1}}, \quad (4)$$

$$D\bar{T}N_N = 0, \quad (5)$$

$$D\bar{T}D_N = 1, \quad (6)$$

$$T\bar{D}D_{-1} = 1, \quad (7)$$

$$T\bar{D}N_{-1} = 0, \quad (8)$$

$$T\bar{D}D_{k-1} = (\mu_{k-1}\bar{\alpha}_k + \mu_k\bar{\alpha}_{k-1})T\bar{D}D_{k-2} + (\mu_{k-1}\bar{\alpha}_k - \mu_k\bar{\alpha}_{k-1})T\bar{D}N_{k-2}e^{-2\bar{\alpha}_{k-1}d_{k-1}}, \quad (9)$$

$$T\bar{D}N_{k-1} = (\mu_{k-1}\bar{\alpha}_k - \mu_k\bar{\alpha}_{k-1})T\bar{D}D_{k-2} + (\mu_{k-1}\bar{\alpha}_k + \mu_k\bar{\alpha}_{k-1})T\bar{D}N_{k-2}e^{-2\bar{\alpha}_{k-1}d_{k-1}}. \quad (10)$$

Coefficients described in (3)-(10) define a recursive function dependent on the earth layer and positions of conductors i and j, which determines the final form of the integrand in (2).

The same expressions are used to compute the self impedance of conductor i using (2), by setting $m = l$ and replacing the horizontal distance with by the conductor effective radius and h_2 with h_1 [5].

The improper integral presented in (2) is solved numerically by using the adaptive quadrature method described in [12].

C. Conductive coupling

The conductive coupling phenomenon relates to the ground potential rise (GPR) caused by current injection into the soil the transmission line or substation grounding electrodes during fault conditions involving the earth, as represented in Fig. 3 [1].

The current flowing into earth through the transmission line grounding conductors, also known as counterpoises, produces a GPR, which appears in the form of voltage gradients around the grounding conductors. If a target structure is within the region affected by the GPR, potentially hazardous voltages may occur.

Conductive EMI is influenced by short-circuit levels, quantity and type of shield wires, distance between the installations, grounding electrode geometry and soil properties [1].

In a previous work [8], the authors proposed an enhanced circuit model to account for conductive coupling in underground conductors. This approach is based on using controlled voltage sources driven by the corresponding Green's functions, as derived by He et al. [6] and Li et al. [7], which accurately express the voltage scalar potentials for N-layered media. Then, each voltage source is controlled by the currents injected into the soil by each tower within the EMI region of interest,

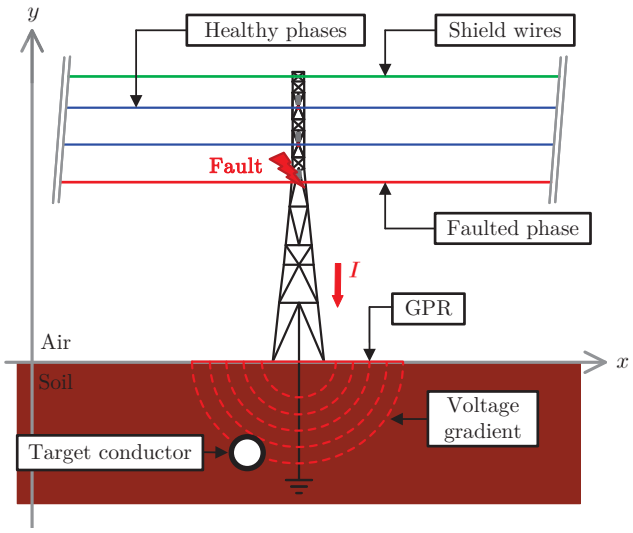

Fig. 3. Conductive coupling phenomenon, adapted from [8].

connected to conductor coating impedance at each circuit node [8].

According to the principle of superposition, the ground potential rise U_P at an observation point O, caused by the sum of all currents I_j injected into the soil at each source point P_j, is given by [7]:

$$U_P = \sum_{j=1}^{N} \hat{G}(P_j, O) \cdot I_j, \quad (12)$$

in which U_P is the potential rise at target point O, in volts; P_j are the spatial coordinates of the j^{th} source point P; and $\hat{G}(P_j, O)$ is a special function that describes the potential produced at point O by a unit point current source located at point P_j, known as Green's function [7], [8].

D. Green's function for N-layered soil

The Green's function representing an earth structure with N horizontal layers is developed in [6], [7]. If the source point is located in the i^{th} layer and the observation point is in the j^{th} layer, then the Green's function general form is written as in (11), in which $r = \sqrt{(x_O - x_P)^2 + (y_O - y_P)^2}$ is the radius in xy plane; $z = z_O - z_P$ is the vertical distance between points O and P; $\hat{\sigma}_j = \sigma_0 + i\omega\epsilon_j$ is the complex conductivity of the j^{th} layer, in siemens per meter; $\hat{J}_0$ is the Bessel function of the first kind and order zero; and $\delta(ij)$ is the Kronecker delta, defined as equal to 1 if $i = j$ and to 0 otherwise [7].

Green's function coefficients $A_{i,j}$ and $B_{i,j}$ are determined by the boundary conditions between surrounding earth layers, including the air layer above the soil surface (0-layer) and the deepest soil layer (N-layer), which are given as:

$$\hat{G}_{i,j-1}(r,z)|_{z=H_{j-1}} = \hat{G}_{i,j}(r,z)|_{z=H_{j-1}}, \quad (13)$$

$$\hat{G}_{i,j}(P,O) = \frac{1}{4\pi\hat{\sigma}_j}\left(\int_0^\infty A_{i,j}(\lambda)\hat{J}_0(\lambda r)e^{-\lambda z}d\lambda + \int_0^\infty B_{i,j}(\lambda)\hat{J}_0(\lambda r)e^{\lambda z}d\lambda + \int_0^\infty \delta(ij)\hat{J}_0(\lambda r)e^{-\lambda|z|}d\lambda\right) \quad (11)$$

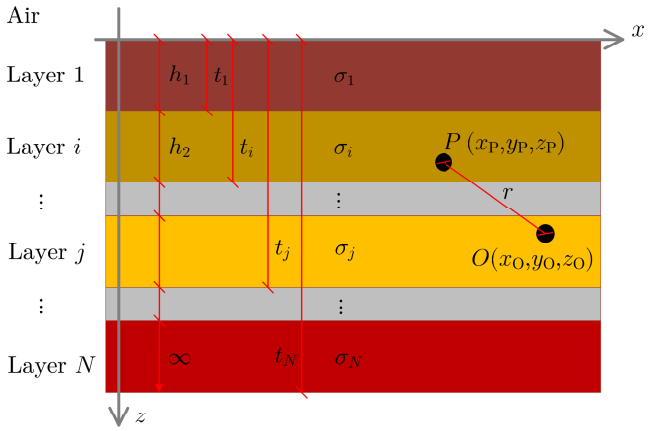

Fig. 4. Point source at i^{th} layer with observation point at j^{th}.

$$\hat{\sigma}_{j-1}\frac{\partial\hat{G}_{i,j-1}(r,z)}{\partial z}\bigg|_{z=H_{j-1}} = \hat{\sigma}_j\frac{\partial\hat{G}_{i,j}(r,z)}{\partial z}\bigg|_{z=H_{j-1}}, \quad (14)$$

$$\hat{G}_{i,N}(r,z)|_{z\to\infty} = 0, \quad (15)$$

$$\frac{\partial\hat{G}_{i,0}(r,z)}{\partial z}\bigg|_{z\to-\infty} = 0, \quad (16)$$

in which $i = 1, 2, \ldots, N$ and $H_0 = 0$. With the appropriate coefficients available, integrals in (11) are solved numerically using adaptive quadratures [12]. In reference [8], Appendix A, it is provided a computer program devised to parse soil stratification data provided by the user and to compute the Green's functions values for arbitrary multilayered horizontal soils by employing the described methods.

E. Stress voltage

An underground conductor close to a transmission line is subjected to two distinct electromagnetic effects under fault conditions, due to inductive and conductive couplings taking place simultaneously. The total voltage transferred to the interfered conductor is the potential difference between the inner metal and the external GPR, or [13]:

$$V_S = E_T - U_P, \quad (17)$$

in which V_S is the total stress voltage, in volts; E_T is the potential of the target conductor resulting from inductive coupling, in volts; and U_P is the local earth potential rise, in volts.

III. Case Description

Fig. 5 illustrates a 1.2 km shared right-of-way composed by a 138 kV transmission line and an underground pipeline, in an industrial area of São Paulo, Brazil. Under nominal load conditions, the double-circuit transmission line is energized with ABC/ABC sequence, frequency 60 Hz and current of 780 A per phase. In the EMI region of interest, the transmission line is composed of 13 towers, each of which with grounding resistances of 15 Ω, and two terminal substations, with grounding resistances of 1 Ω. The transmission line side view and the conductor coordinates are displayed in Fig. 6.

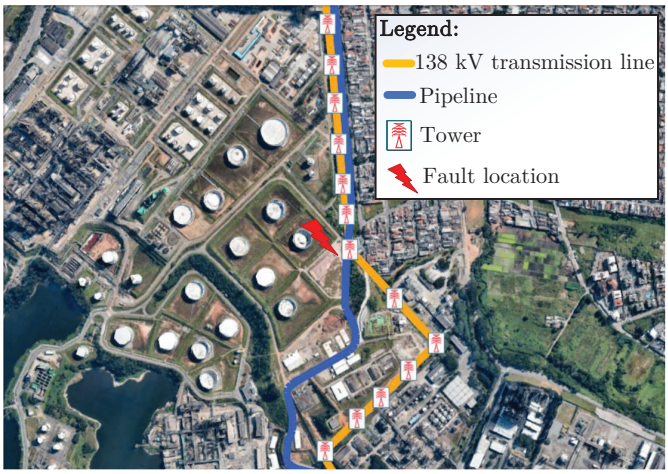

Fig. 5. Shared right-of-way between a transmission line and a pipeline in Brazil.

The underground pipeline is constructed in 14" diameter carbon steel and buried 1.2 meters within the ground. The pipeline is grounded at its extremities through 10 Ω resistances. The characteristics of the transmission line conductors and the pipeline are presented in Table I.

TABLE I
Specification and Characteristics of System Conductors

Conductor	r_{out} [m]	r_{in} [m]	$R_{DC}[\Omega/km]$
ACSR Grosbeak	0.0125705	0.0046355	0.0924806
Steel 3/8" EHS-CG	0.004572	-	3.42313
Pipe 14"	0.1778	0.168275	0.099516

The soil is modeled as a 3-layered structure based on apparent resistivity measurements performed at the right-of-way location. The specifications of the layer resistivities and thicknesses are given in Table II.

IV. Case Study Under Nominal Load Conditions

First, a simple EMI inductive study is carried out in order to demonstrate the validity of the proposed circuit model.

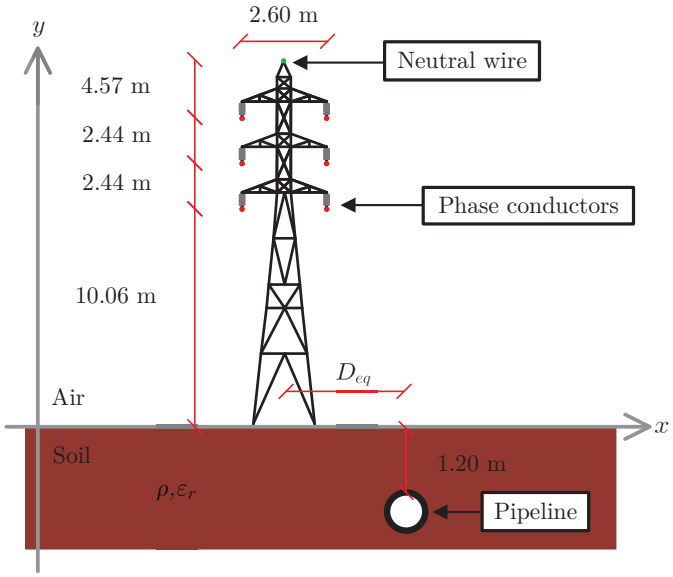

Fig. 6. System cross-section.

TABLE II
SOIL PARAMETERS

Layer	Resistivity [Ω.m]	Thickness [m]
1	488.71	1.73
2	2074.66	8.99
3	451.41	∞

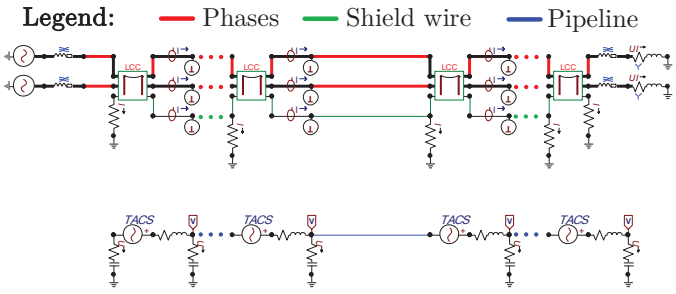

Fig. 7. Nominal load EMTP simplified model representation.

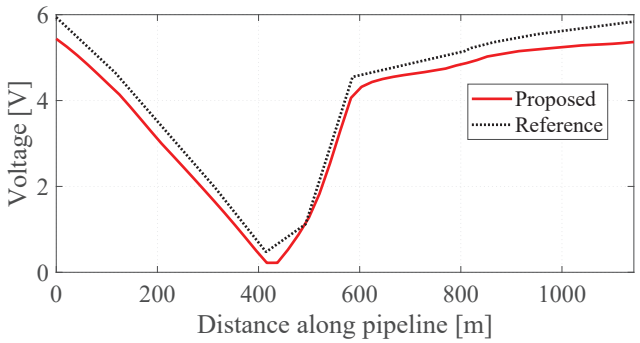

Fig. 8. Induced voltage along the pipeline under nominal load conditions.

A. Nominal load EMTP equivalent circuit

Due to the system geometry being composed of obliquities, crossings and parallelisms, the right-of-way is subdivided into smaller sections and, for each subdivision, it is calculated a parallel equivalent segment, as described in detail in [14]. The transmission line is modeled in the EMTP/ATP as a series of Line Constants (LCCs) objects, which are constructed with the corresponding parallel segment parameters. Fig. 7 presents the simplified circuit used for inductive simulations under nominal load conditions, in which the objects labeled as TACS are the controled voltage sources native of ATP, representing the sum of the EMFs produced by phase conductors and shield wires. The current probes of the TACS sources are placed to measure the series current at each LCC output terminal and the current values are used to build the EMF sources distributed along the interfered conductor, represented in the inferior part of Fig. 7.

B. Nominal load simulation results

Fig. 8 shows the induced voltage along the pipeline using the proposed model, as well as the comparison with the EMI reference software CDEGS [15].

Results show that the proposed model agrees with the reference software, presenting an RMS error of 7.35%, which is mainly explained by the different line models and impedance formulations used in each approach.

Due to the grounding resistance at the pipeline extremities, the induced voltage does not exceed the safety limit of 15 V in steady-state regime [16]. Grounding resistances provide a safe path to the induced currents flow back into the earth, thus preventing risks to the interfered installation.

As the proposed circuit model is considered to be validated, the next section follows with the simulation of a more complex scenario, consisting of a possible fault situation and its impacts on the nearby pipeline.

V. Case Study Under Fault Conditions

In order to study the ground potential rise and the total stress voltage, a phase-to-ground fault is applied to the system presented in Section III.

A. Fault regime EMTP equivalent circuit

The phase-to-ground fault is assumed to occur at tower #7. A resistance value of 0.001 Ω is chosen to represent a short-circuit between the phase B conductor and the shield wire.

Fig. 9 shows the simplified equivalent circuit for fault simulations. The model is constructed by following the same procedure described in the preceding section. However, additional TACS sources are connected to the pipeline coating impedance to represent the ground potential rise due to conductive coupling. The current probe of the TACS sources measures the current flowing through each tower grounding impedance to the local earth.

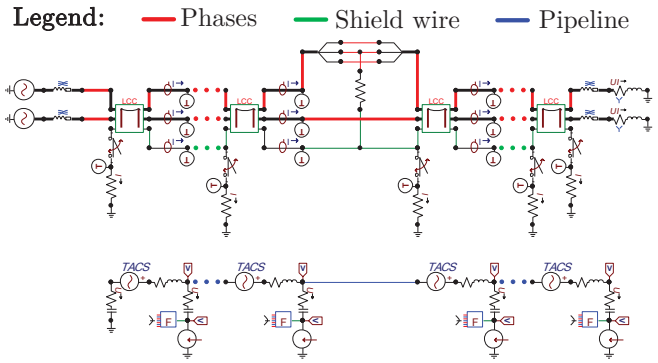

Fig. 9. EMTP simplified model representation for fault regime study.

B. Fault condition simulation results

The potential resulting from inductive coupling, the local ground potential rise and the resulting stress voltage distribution due to the phase-to-ground fault simulated are presented in Fig. 10.

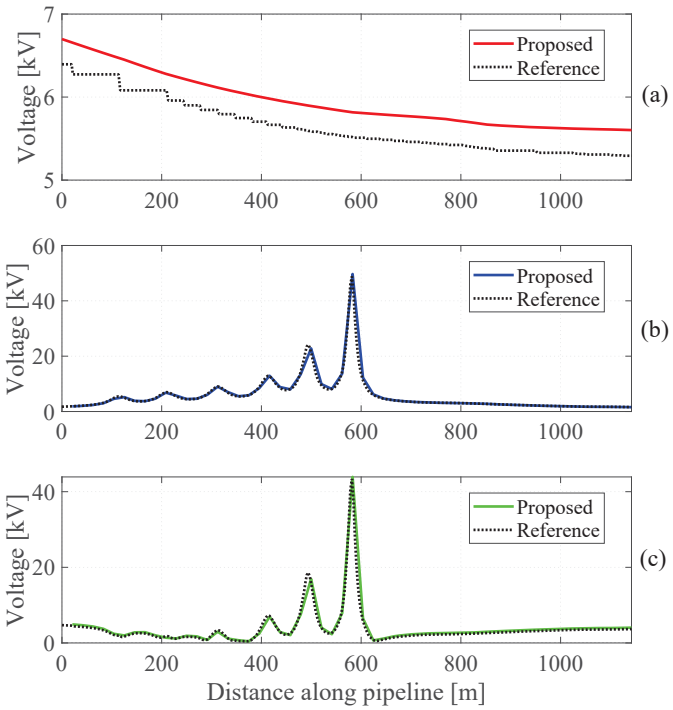

Fig. 10. Pipeline voltage due to: (a) inductive coupling; (b) GPR; and (c) total stress.

The obtained results agree with the reference software, with RMS errors of 1.42% and 1.21%, respectively. The inductive voltage presented a RMS error of 21.17%. However, since both curves present the same shape with a nearly constant offset, it is relevant to observe also the average relative error. In this case, the inductive coupling voltage presents a deviation of 5.5%.

The total stress voltage along the pipeline reaches 43.9 kV close to the fault location, which may cause dielectric breakdown of the coating layer, exposing the metal to electrochemical corrosion [16]. Modern pipeline coating materials, such as the 3-Layer Polyethylene (3LPE), are designed to withstand voltages up to 25 kV, according to manufacturer's information [16].

Fig. 11 shows the currents flowing in the shield wires and through the tower groundings. The largest values occur in the vicinities of the faulted tower, which justifies the shape of the GPR curve shown in Fig.10-b.

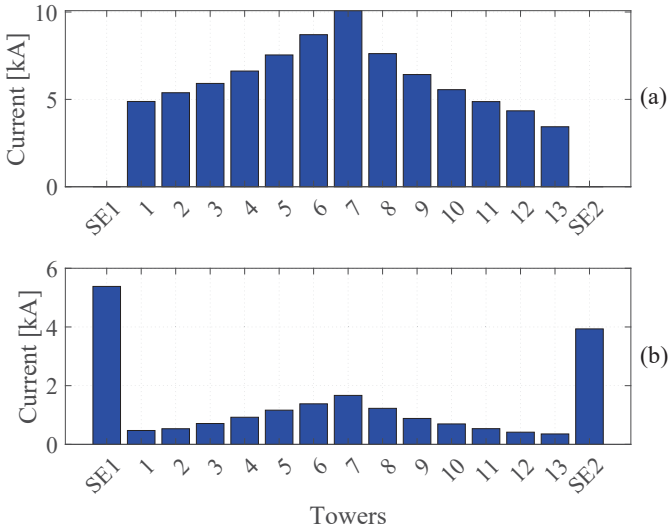

Fig. 11. (a) Ground currents; and (b) currents flowing through the shield wire.

VI. Mitigation Study

As the total stress under fault conditions far exceeds safety limits, which may present risks to the pipeline integrity, a mitigation design is proposed. The proposed mitigation consists of connecting the pipeline to the earth at regularly-spaced points using an adequately sized grounding conductor ($\leq 10\ \Omega$). This method is used to transfer the external ground potential rise to the inner metal, thus reducing the difference in (17) and, consequently, decreasing the resulting stress voltages.

In the case shown in this paper, the hazardous region is located from 450 to 650 meters along the pipeline path. Within this zone, the pipeline is grounded at every 40 m through 1 Ω resistors. Fig. 12 presents the comparison between the pipeline voltages before and after the mitigation.

Is observed that the proposed mitigation design reduces the maximum stress voltage to 21 kV, thus meeting the safety criteria adopted in pipeline industry [16].

It is important to notice that the mitigation method is efficient to reduce the stress voltages in the intended location. However, for regions outside the mitigation influence, the pipeline potential may rise. This is related to the inner pipeline voltage reaching 33 kV, approximately 6.6 times superior to

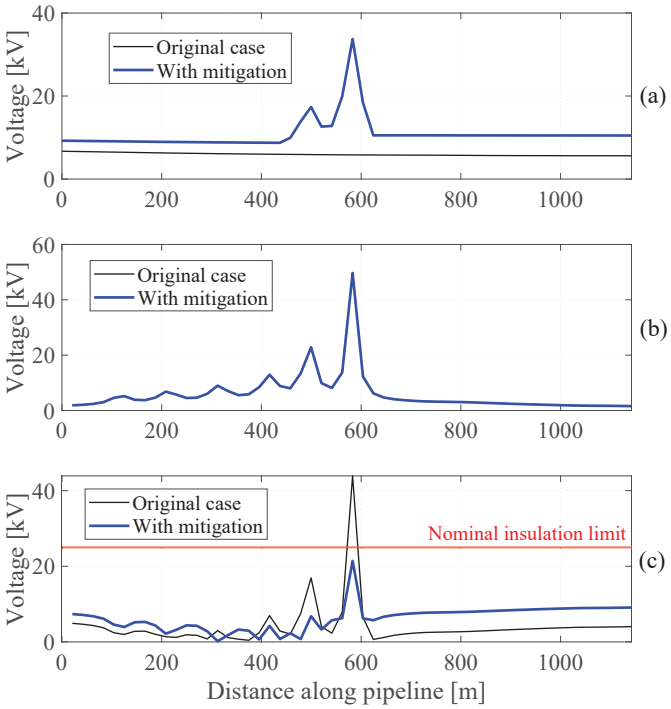

Fig. 12. Comparison of pipeline voltages before and after the mitigation due to: (a) inductive coupling; (b) GPR; and (c) total stress.

the original case, which is exactly the equipotential condition sought in grounding designs.

VII. Conclusions

This work presented an EMTP-based circuit approach to predict total stress voltages in a pipeline due to a transmission line phase-to-ground faults. The proposed method is based on formulations which effectively represent multilayered soils without approximations or uniform equivalents.

To validate the proposed methodology, a real case of right-of-way shared between an underground pipeline and a double-circuit 138 kV transmission line was modeled and tested, under nominal and fault conditions.

Results showed that the methodology is valid and accurate under both nominal and fault condition scenarios, presenting a maximum error of 7.35% in comparison with EMI analysis industry-standard software.

Under nominal conditions, the maximum induced voltage reached 6 V, being considered a safe value to the facilities and personnel involved. However, under phase-to-ground fault conditions, the stress voltage reached almost 44 kV, which may be hazardous for the pipeline coating and without conformity with the nominal limits established for the industry.

For this reason, further studies were carried out and a mitigation was designed to handle the case under study. The method consisted of grounding the pipeline along the hazardous zone. The results obtained proved that the mitigation method is efficient, having decreased the original voltages in 47%, leading the final stress to below the 25 kV safe limit.

This work offered relevant insights of how resourceful the EMTP-based EMI simulation techniques can be when applied to problems of practical relevance to the industry, especially when one is concerned with the safety of facilities and personnel involved.

Acknowledgment

This work was developed in partnership with IATI and CEPEL within the scope of the R&D project PD-06908-0003/2021, sponsored by the Brazilian Agency of Electrical Energy (ANEEL) and EVOLTZ. The authors thank the cooperation of Ms. Larissa Silva (EVOLTZ) and Dr. Marco Antônio M. Rodrigues (CEPEL).

References

[1] CIGRÉ WG-36.02, "Technical Brochure n. 95 - Guide on the Influence of High Voltage AC Power Systems on Metallic Pipelines," Paris, pp. 1–135, 1995.

[2] L. Qi, H. Yuan, L. Li, and X. Cui, "Calculation of Interference Voltage on the Nearby Underground Metal Pipeline due to the Grounding Fault on Overhead Transmission Lines," *IEEE Transactions on Electromagnetic Compatibility*, vol. 55, no. 5, pp. 965–974, 2013.

[3] X. Wu, H. Zhang, and G. G. Karady, "Transient analysis of inductive induced voltage between power line and nearby pipeline," *International Journal of Electrical Power and Energy Systems*, vol. 84, no. January, pp. 47–54, 2017. [Online]. Available: http://dx.doi.org/10.1016/j.ijepes.2016.04.051

[4] M. Alexandru, L. Czumbil, D. D. Micu, and T. Papadopoulos, "Analysis of Electromagnetic Interferences between AC High Voltage Power Lines and Metallic Pipeline Using Two Different Approaches Based on Circuit Theory and Electromagnetic Field Theory," *EPE 2020 - Proceedings of the 2020 11th International Conference and Exposition on Electrical And Power Engineering*, pp. 519–524, 2020.

[5] D. A. Tsiamitros, G. K. Papagiannis, P. S. Dokopoulos, and A. E. F. Equations, "Earth Return Impedances of Conductor Arrangements in Multilayer Soils - Part I : Theoretical Model," *IEEE Transactions on Power Delivery*, vol. 23, no. 4, pp. 2392–2400, 2008.

[6] J. He, R. Zeng, and B. Zhang, *Methodology and Technology for Power System Grounding*. Wiley, 2012.

[7] Z.-X. Li, J.-B. Fan, and W.-J. Chen, "Numerical simulation of substation grounding grids buried in both horizontal and vertical multilayer earth model," *International Journal for Numerical Method in Engineering*, no. February, pp. 1102–1119, 2006. [Online]. Available: http://onlinelibrary.wiley.com/doi/10.1002/nme.3279/full

[8] A. G. Martins-Britto, "Realistic Modeling of Power Lines for Transient Electromagnetic Studies," Ph.D. dissertation, University of Brasília, 2020. [Online]. Available: https://www.researchgate.net/publication/342916469_Realistic_Modeling_of_Power_Lines_for_Transient_Electromagnetic_Interference_Studies

[9] J. R. Carson, "Wave Propagation in Overhead Wires with Ground Return," *Bell System Technical Journal*, vol. 5, no. 4, pp. 539–554, 1926.

[10] M. Nakagawa, A. Ametani, and K. Iwamoto, "Further Studies on Wave Propagation in Overhead Lines with Earth Return: Impedance of Stratified Earth," *Proceedings of the Institution of Electrical Engineers*, vol. 120, no. 12, p. 1521, 1973. [Online]. Available: https://digital-library.theiet.org/content/journals/10.1049/piee.1973.0312

[11] F. Pollaczek, "On the Field Produced by an Infinitely Long Wire Carrying Alternating Current," *Electrische Nachrictentechnik*, vol. III, no. 9, pp. 339–359, 1926.

[12] L. F. Shampine, "Vectorized adaptive quadrature in MATLAB," *Journal of Computational and Applied Mathematics*, vol. 211, no. 2, pp. 131–140, 2008.

[13] IEEE Std 80, "Guide for Safety In AC Substation Grounding," pp. 1–192, 2000.

[14] C. M. Moraes, A. G. Martins-Britto, and F. V. Lopes, "Electromagnetic Interferences Between Power Lines and Pipelines Using EMTP Techniques," *WCNPS 2020: 5th Workshop on Communication Networks and Power Systems*, 2020.

[15] F. Dawalibi and C. Blattner, "Earth Resistivity Measurement Interpretation Techniques," *IEEE Transactions on Power Apparatus and Systems*, vol. PAS-103, no. 2, pp. 374–382, 1984. [Online]. Available: http://ieeexplore.ieee.org/lpdocs/epic03/wrapper.htm?arnumber=4112522

[16] NACE International, *Mitigation of Alternating Current and Lightning Effects*, 2007, vol. SP0177.